Journal of Chromatography A, 1217 (2010) 7231–7241

Contents lists available at ScienceDirect

Journal of Chromatography A

journal homepage: www.elsevier.com/locate/chroma

Characterization and optimization by experimental design of a liquid chromatographic method for the separation of hydroxylated polychlorinated biphenyls on a polar-embedded stationary phase

Jesús Eduardo Quintanilla-López[a], Plácido Galindo-Iranzo[b], Belén Gómara[a], Rosa Lebrón-Aguilar[b,*]

[a] Institute of General Organic Chemistry (CSIC), Juan de la Cierva 3, 28006 Madrid, Spain
[b] Institute of Physical Chemistry "Rocasolano" (CSIC), Serrano 119, 28006 Madrid, Spain

ARTICLE INFO

Article history:
Received 13 July 2010
Received in revised form 8 September 2010
Accepted 9 September 2010
Available online 17 September 2010

Keywords:
Hydroxylated polychlorinated biphenyls
Liquid chromatography
Polar embedded stationary phases
Experimental design
Retention modeling

ABSTRACT

Traditionally, the determination of hydroxylated polychlorinated biphenyls (OH-PCBs) has been carried out by gas chromatography (GC). However, the gas chromatographic behavior and sensitivity of this type of hydroxylated compounds are not always satisfactory, hence a prior derivatization of the OH-PCBs must be performed. Therefore, the development of liquid chromatographic methods should prove to be a very interesting task aimed at dealing with the instrumental determination of OH-PCBs. Taking into account that octadecylsilane stationary phases are not the most adequate for the separation of isobaric compounds, an amide-type column has been tested. For the development of the method, the Response Surface Methodology was used, based on a Box–Wilson Central Composite experimental design. The initial content of methanol in the mobile phase, the gradient time, and the concentration and the pH value of the buffer were chosen as relevant experimental parameters. A global optimum was obtained by selecting the elution time, the sensitivity and the overall resolution as responses to optimize. The developed method for liquid chromatography presented a very good resolution and sensitivity, and a reasonably short analysis time. In addition, a retention study was conducted in order to survey the different interactions that take place in the separation process, showing that hydrogen bonding is the main interaction between OH-PCBs and the amide-type stationary phase. However, a substantial contribution of dispersion forces was present in methanol contents in the mobile phase below 65%. Besides, the pH value of the mobile phase was found to be the most important parameter to control the hydrogen bond forces and therefore, to regulate the OH-PCBs separation.

1. Introduction

Polychlorinated biphenyls (PCBs) are a group of ubiquitous pollutants that are usually present in environmental and biological samples as complex mixtures [1]. In general, PCBs, in the same way as other persistent organic pollutants, are metabolized leading to polar metabolites which are supposed to be more easily excreted. Particularly, in a living organism, PCBs are initially metabolized by hepatic microsomial oxidases to their corresponding hydroxylated metabolites (OH-PCBs) which are eliminated mainly via the bile [2]. However, some studies have shown that OH-PCB metabolites can be bound to specific plasma proteins, being retained and accumulated in different species [3–5]. In addition, some authors have established that OH-PCBs present agonist or antagonist interactions with hormone receptors and/or induce hormone–receptor-mediated responses [6,7]. Thus, nowadays, it is still not clear if PCB toxicity is only due to their concentrations or whether it is also due to the presence of PCB metabolites in the same individual [8]. All the indications above demonstrate that PCB metabolites should be considered as a secondary class of contaminants of concern.

OH-PCBs are usually determined by gas chromatography (GC), with electron capture detectors (ECD) or coupled to mass spectrometry (MS) [9]. However, a previous derivatization of the OH-PCBs into their methoxylated [10], propylated [11] or pentafluorobenzoyl derivates [12] is mandatory for obtaining enhanced chromatographic properties and sensitivity by GC. In order to avoid this extra step, the development of liquid chromatographic methods should become a useful analytical tool for the separation of these new contaminants. At the moment, there are few studies that use liquid chromatography (LC) for OH-PCB separation and almost all of them employ octadecylsilane stationary phases (hereafter ODS-type) [13–15]. Nevertheless, the separation obtained is not always satisfactory, since it is driven by hydrophobic interac-

* Corresponding author. Tel.: +34 91 7459544; fax: +34 91 5642431.
E-mail address: rlebron@iqfr.csic.es (R. Lebrón-Aguilar).

0021-9673/$ – see front matter © 2010 Elsevier B.V. All rights reserved.
doi:10.1016/j.chroma.2010.09.032

tions. As a consequence, those compounds with the same moiety are mainly separated in order of their increasing molecular mass, frequently leading to coelution of isobaric compounds [15] which cannot be distinguished from their mass spectra.

A better approach would be the use of chromatographic columns with stationary phases (SPs) which show a greater selectivity towards this type of compound. Especially suitable are those SPs with a polar embedded group [16–21], because these polar groups could promote hydrogen bonds with the hydroxyl group of the OH-PCBs, a very intense and selective interaction force. These SPs, initially introduced to improve the elution of basic compounds [22], are being increasingly used, because of their very particular selectivity, low activity of the superficial silanol groups, good reproducibility, good compatibility with mass spectrometers, and their ability to work with highly aqueous mobile phases. Among these SPs, those with an amide group embedded into an alkyl chain show an especially high affinity towards substances capable of giving hydrogen bonds, as has been stated in several comparative studies and applications [23–28]. The increasing interest in these SPs has even lead to in-depth study by simulation processes of the interaction forces that they are able to produce [29,30].

On the other hand, even having the right chromatographic column for a given separation, it is not a simple task to find optimal analytical conditions due to the large number of variables involved in the separation process. For this reason it is usually more effective and time saving to resort to experimental design procedures [31–33], and especially to the so-called Response Surface Methodology. As a preliminary step, this methodology requires some screening experiments to be carried out in order to establish the significant experimental factors, and also to determine the upper and lower levels for these factors, in an attempt to reach values near to the optimal response.

Therefore, the objective of this work is to develop and optimize a liquid chromatographic method for the separation of OH-PCBs on a stationary phase with an embedded amide group, by means of experimental design. Moreover, a deeper insight into the chromatographic behavior of the OH-PCBs on this type of SP is obtained.

2. Experimental

2.1. Reagents and standards

Methanol of LC–MS Chromasolv® grade and ammonium formate (purity ≥ 99.0%) were supplied by Sigma–Aldrich (St. Louis, MO, USA). Milli-Q water was obtained using a Millipore system (Billerica, MA, USA). The OH-PCBs standards, gathered in Table 1, were purchased from Cambridge Isotope Laboratories (Andover, MA, USA). Formic acid (98–99% purity) was supplied by Merck Co. (Darmstadt, Germany).

2.2. Apparatus

All the LC–MS experiments were carried out on a Finnigan Surveyor pump with quaternary gradient system coupled to a Finnigan LCQ Deca ion trap mass spectrometer using an ESI interface, all from Thermo Fisher Scientific (Waltham, MA, USA).

For MS experiments spray voltage was set at 4.5 kV and heated capillary temperature at 275 °C. Nitrogen (99.5% purity) was used as sheath (0.6 L min^{-1}) and auxiliary (6.0 L min^{-1}) gas, and helium (99.9990% purity) was used as the collision gas. Mass spectra were acquired in the negative selected ion mode (SIM) monitoring the $[M-H]^-$ ions of the studied OH-PCB congeners, that is the m/z ratios 341.2 (OH-penta-CBs), 375.2 (OH-hexa-CBs), 387.2 (labeled 4′-OH-CB159) and 409.1 (OH-hepta-CBs), using a span of six mass units, in order to record the most intense ions in their isotopic clusters. Optimization of ion transmission into the ion trap was performed by infusing a methanolic solution of 3′-OH-CB138 (500 pg μL^{-1}) into the mass spectrometer at a flow rate of 5 μL min^{-1} using the syringe pump included in the LCQ instrument and mixing it with 100 μL min^{-1} of methanol:water:formic acid 5%, (90:8:2, v/v/v) by means of a zero-dead volume T-piece.

The LC experiments were performed on three different columns: a polar embedded column HyPurity Advance (100 mm × 2.1 mm, 3 μm), an octadecylsilane (ODS) reverse phase column HyPurity C18 (100 mm × 2.1 mm, 3 μm), both purchased from Thermo Fisher Scientific (Hypersil Division, Cambridge, UK), and an ODS column Ascentis C18 (150 mm × 2.1 mm, 3 μm) from Supelco (St. Louis, MO, USA). Injections of 10 μL of a mixture of the OH-PCB standards (50 pg μL^{-1}) were carried out. The solvent composition for this mixture was adapted to have the same composition as the initial mobile phase used in each LC run. For the optimization process, different elution programs were assayed (see Section 3.2), containing variable percentages of water (eluent A) and methanol (eluent B), and 2% of formate ammonium (eluent C). Initial conditions were always maintained for 2 min after which the percentage of eluent B was linearly increased to 98%, this value being maintained until complete elution of the compounds was obtained. Then, the program ramped to the original composition in 1 min and equilibrated for 15 min.

The column hold-up time (t_M) was determined by using an aqueous solution of potassium bromide (0.1%, w/v) as unretained solute. Retention data were expressed by the logarithm of the retention factor, $\log k$, defined as $\log k = \log[(t_R - t_M)/t_M]$ where t_R is the retention time of the solute. All the measurements were taken in triplicate.

The determinations of pH values were carried out using a Thermo Orion 410A pH meter, provided with a 91-04 combined glass pH electrode with an Ag/AgCl internal reference system (Thermo Fisher Scientific). The pH meter was calibrated using aqueous buffers of pH 4.01 and 7.00. Values of pH were taken in aqueous and in hydro-organic solutions. For the sake of clarity, pH and pK_a values measured in hydro-organic solvents are referred to as ${}^{s}_{w}$pH and ${}^{s}_{w}$pK_α [34,35] respectively, while these parameters measured in pure water are represented simply by pH and pK_a.

2.3. Data treatment and experimental design

The LC–MS system, data acquisition and processing were managed by Xcalibur 1.2 software (Thermo Fisher Scientific). Microsoft EXCEL 2007 utility (Microsoft Corp., Redmond, WA, USA) was used for calculations and the Statgraphics Centurion XV program (Statpoint Technologies Inc., Warrenton, VA, USA) for experimental design and statistical data analysis.

Experimental design was carried out by applying Response Surface Methodology (RSM), widely used for process optimization [36–42]. This methodology allows optimization of analytical methods by carrying out a relatively small number of experiments and with no prior knowledge of interaction forces between analytes and stationary phase [43–45]. Although a number of RSM procedures are available, Box–Wilson Central Composite Design was chosen due to its widespread use and versatility [46–50]. This procedure consists of a factorial design together with center and star points that allow the evaluation of the relationship of a set of controlled experimental factors and observed results. This optimization process involves three major steps, namely, performing the statistical design experiments, estimating the coefficients of the mathematical model according to Eq. (1), and predicting the response in order to check the adequacy of the model.

$$Y_{X,t} = \beta_0 + \sum_{i=1}^{n} \beta_i x_i + \sum_{i=1}^{n} \beta_{ii} x_i^2 + \sum_{i<j} \beta_{ij} x_i x_j + \varepsilon_{X,t} \quad (1)$$

Table 1
Characteristics of the OH-PCB congeners selected.

#	IUPAC name	Short name	M_r	Structure
1	2,3,3′,4′,5-pentachloro-[1,1′-biphenyl]-4-ol	4-OH-CB107	339.878	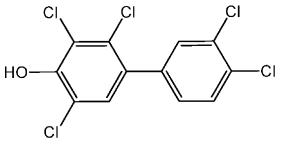
2	2′,3,3′,4′,5-pentachloro-[1,1′-biphenyl]-4-ol	4′-OH-CB108	339.878	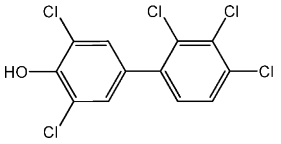
3	2,3′,4,4′,5-pentachloro-[1,1′-biphenyl]-3-ol	3-OH-CB118	339.878	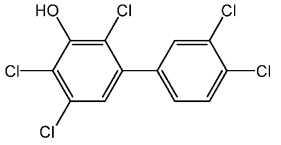
4	2,2′,3′,4,4′,5-hexachloro-[1,1′-biphenyl]-3-ol	3′-OH-CB138	373.839	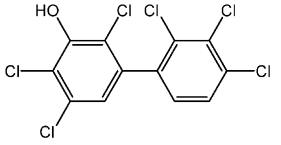
5	2,2′,3,4′,5,5′-hexachloro-[1,1′-biphenyl]-4-ol	4-OH-CB146	373.839	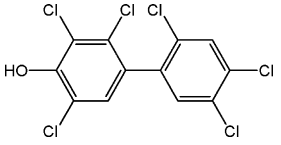
6	2′,3,3′,4′,5,5′-hexachloro-[1,1′-biphenyl]-4-ol[a]	4′-OH-CB159	373.839	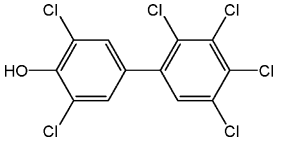
7	2,2′,3,3′,4′,5,5′-heptachloro-[1,1′-biphenyl]-4-ol	4′-OH-CB172	407.800	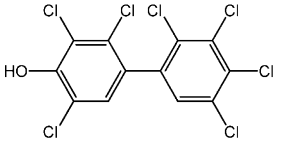
8	2,2′,3′,4,4′,5,5′-heptachloro-[1,1′-biphenyl]-3-ol	3′-OH-CB180	407.800	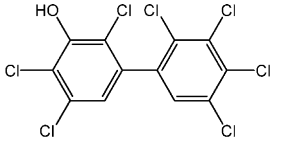
9	2,2′,3,4′,5,5′,6-heptachloro-[1,1′-biphenyl]-4-ol	4-OH-CB187	407.800	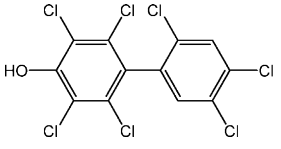

[a] Labeled with twelve ^{13}C atoms and used as internal standard.

where n is the number of factors, $Y_{X,t}$ denotes the t^{th} response observed for combination $X=(x_1, x_2, \ldots, x_n)$, and $\varepsilon_{X,t}$ the random-error variables. The parameter β_i represents the linear effect of the i^{th} factor. The parameter β_{ii} represents the quadratic effect of the i^{th} factor, and β_{ij} represents the cross-product effect, or interaction effect, between the i^{th} and j^{th} factors. In order to estimate the parameters in Eq. (1), the experimental design must ensure that all the studied variables are examined on at least three factor levels.

2.4. Molecular parameter calculation

The estimation of pK_a values was achieved by using the online program SPARC 4.5 [51], not only because of the reliability of its calculations, but also for its easy and free access [52]. The ${}^{s}_{w}pK_{\alpha}$ values for each compound were calculated at different MeOH:H_2O ratios, since they will vary according to the composition of the mobile phase [34,53]. Finally, the log D was obtained with Eq. (2), using the ${}^{s}_{w}pK_{\alpha}$ values previously calculated, the ${}^{s}_{w}$pH values of each elu-

Table 2
Chromatographic factors used for the Box–Wilson Central Composite Design.

Level	$MeOH_i$ (%, v/v)	G_t (min)	AF (mM)[a]	pH_c[a]
–	40	5.00	5.00	2.0
0	65	17.5	25.0	2.4
+	90	30.0	50.0	2.8

[a] Values in the eluent C, not in the mobile phase.

ent mixture, and the partition coefficient ($\log P$) obtained with the Chembio3D Ultra 12.0 program (CambridgeSoft Corp., Cambridge, MA, USA), by applying the CLogP algorithm.

$$\log D = \log P + \log \frac{1}{1 + 10^{{}^{s}_{w}\mathrm{pH} - {}^{s}_{w}\mathrm{p}K_{\alpha}}} \quad (2)$$

3. Results and discussion

3.1. Preliminary studies

In order to deal with the liquid chromatographic separation of OH-PCBs on a stationary phase with an embedded amide group (hereafter amide-type), a preliminary study was made to establish the most significant variables for the further design of experiments. For this purpose, a few experiments modifying several working parameters were carried out, such as organic solvent (acetonitrile, methanol), additives (different acids and salts), column temperature, and gradient parameters. The best approach was obtained at 25 °C, using a mixture of MeOH:H_2O with a buffer of formic acid/ammonium formate as the eluent.

3.2. Experimental design

Once the preliminary studies were finished, and in order to optimize the chromatographic conditions, a Response Surface Methodology was carried out applying a Box–Wilson Central Composite Design (BWD). The chosen parameters were the initial content of methanol in the gradient ($MeOH_i$), the gradient time (G_t), the ammonium formate concentration (AF) of eluent C and its pH (pH_c). It is important to point out that the AF and pH_c values were measured in the eluent C, not in the mobile phase, which only contains 2% of that eluent. Table 2 shows the different experimental levels used in the BWD. The total number of experiments was 30, including face centered points and 8 replicates of the central point, with the purpose of obtaining a good estimation of the experimental variability. Factor levels for each design point are detailed in Table 3.

The next step in the optimization process was to set the most relevant characteristics for the chromatographic results. As is usual in this type of analysis, a multicriteria approach to reach the best separation with a short analysis time and a high sensitivity was followed. In this regard, the Derringer's desirability function (D_f) [54–56] was chosen, because it allows the simultaneous optimization of several goals, showing user flexibility in its definition. The retention time of the last eluted compound (4-OH-CB187) was taken as the analysis time (t_a) indicator, and the area summation (ΣA) corresponding to all the OH-PCBs was chosen to evaluate the overall sensitivity. Finally, with the purpose of obtaining the best global resolution (R_{SG}) we tried to maximize the value of the geometric average of the resolutions between consecutive peaks, calculated according to the following expression:

$$R_{SG} = \left(\prod_{i=1}^{n-1} R_{S_i}\right)^{1/(n-1)} = \sqrt[n-1]{R_{S_1} R_{S_2} \cdots R_{S_{(n-1)}}} \quad (3)$$

where R_{si} is the resolution between two consecutive chromatographic peaks, and n is the number of compounds taken into account to calculate the average resolution. For this calculation, the 4-OH-CB187 was not considered, since it was the last eluted compound, with no overlapping problems. The values obtained for D_f and the experimental responses are gathered in Table 3.

Fig. 1 shows the standardized Pareto bar charts resulting from the BWD carried out. In these graphs, the degree of influence of every variable in the model, as well as their combinations up to a second order level, can be easily visualized. Furthermore, the positive (blue bar) or negative (red bar) effect on the selected response is also indicated. The vertical line represents the confidence level (α) of 0.05, so that the variables whose bars exceed this line will be those with a greater degree of statistical meaning in the model.

Thus, for R_{SG} (Fig. 1(a)) the two more influential variables are $MeOH_i$ and pH_c, but with opposite effects, since R_{SG} decreases when increasing $MeOH_i$ but increases when the value of pH_c rises. In addition to these two variables, some others also have a relevant effect on the resolution, specially AF and the effect of second order [(AF)(pH_c)], both with a negative effect on the resolution. Moreover, beneath but very close to the value of $\alpha = 0.05$, the effect of G_t is found as well as many other second order effects. Therefore, a complex dependency of R_{SG} on the different studied variables exists, clearly shown in Fig. 1(d), where it can be observed that there is a second order variation in all the cases, presenting, moreover, a maximum within the working interval for $MeOH_i$ and G_t, and a minimum for AF. In order to really understand this behavior, a more detailed study of the retention process for these compounds in the amide-type column was considered interesting and useful (see Section 3.3).

With regards to t_a, the Pareto charts (Fig. 1(b)) show that all the studied variables affect it significantly, namely, positive in case of pH_c and G_t, and negative for the $MeOH_i$ and AF. Furthermore, several second order interactions are also important, especially [(AF)(pH_c)], [$(MeOH_i)^2$] and [($MeOH_i$)(G_t)], all with a negative effect, and [$(AF)^2$] with a positive effect. Nevertheless, the graph of main effects (Fig. 1(e)) is easier to interpret than those of R_{SG}, since plots are less curved, and only a smooth minimum for AF, and a maximum for $MeOH_i$ can be observed.

Finally, as can be seen in Fig. 1(c) the global sensitivity (ΣA) is mainly affected in a negative way by the AF value. In fact, this is not surprising, as the inhibition effect of salts in the electrospray ionization process is well known. The next variable according to importance is the pH_c, producing a moderate increase of sensitivity, probably due to its influence on the ionization state of the OH-PCBs. The effect of the rest of the variables is well below $\alpha = 0.05$. In the graph of main effects (Fig. 1(f)) a maximum is observed for $MeOH_i$, which can be explained by the relationship existing between the mobile phase composition and the efficiency of spray generation, usually optimal for moderate contents of organic modifier. The variation of sensitivity against G_t shows a minimum around the middle point of the tested range, probably related to a number of factors such as chromatographic peak shape and ionization efficiency.

In order to give a global view and clarify the behavior of the model obtained from the experimental design, Fig. 2 shows the response surfaces for all the possible pairs of variables. In each case, the other two variables not considered are set at their optimum value obtained from the BWD. According to these graphs the D_f values tend to show a smooth behavior in all the cases, since for all the variable combinations a relatively broad area exists with values near to the optimum. This is an advantageous characteristic, because it implies a robust analytical method and therefore good precision can be expected. Furthermore, it can be seen that the experimental conditions that clearly produce the worst values of D_f are the combinations of high $MeOH_i$, low G_t and low pH_c.

The multicriteria optimization process gave a maximum value of 0.73 for D_f, and the resulting optimum working conditions are to be found at the bottom of Table 3. A good agreement between

Table 3
Factor levels, responses and Derringer's function values for the BWD. Optimal conditions are gathered at the end of the table (see text for symbol meaning).

Design points	Factor levels				Responses			
	$MeOH_i$ (%, v/v)	G_t (min)	AF (mM)[a]	pH_c[a]	R_{SG}	t_a (min)	ΣA (10^7)	D_f
1	40	5.00	5.00	2.80	0.547	45.72	2.67	0.560
2	40	30.0	5.00	2.80	0.689	65.00	2.57	0.000
3	90	5.00	5.00	2.80	0.495	37.66	3.50	0.699
4	90	30.0	5.00	2.80	0.498	39.55	3.33	0.596
5	65	17.5	27.5	2.80	0.268	33.29	2.31	0.571
6	40	5.00	50.0	2.80	0.342	24.47	1.91	0.396
7	40	30.0	50.0	2.80	0.367	42.42	2.23	0.453
8	90	5.00	50.0	2.80	0.236	13.48	1.84	0.400
9	90	30.0	50.0	2.80	0.000	13.02	1.73	0.281
10	65	17.5	5.00	2.40	0.504	37.06	3.39	0.696
11	40	17.5	27.5	2.40	0.367	32.11	2.12	0.454
12	65	30.0	27.5	2.40	0.465	33.31	2.48	0.536
13	65	17.5	27.5	2.40	0.418	27.60	2.73	0.553
14	65	17.5	27.5	2.40	0.386	27.54	2.63	0.553
15	65	5.00	27.5	2.40	0.000	21.15	2.78	0.523
16	65	17.5	27.5	2.40	0.400	22.58	1.46	0.553
17	65	17.5	27.5	2.40	0.479	22.54	1.96	0.553
18	65	17.5	27.5	2.40	0.444	22.83	1.77	0.553
19	65	17.5	27.5	2.40	0.375	23.05	2.01	0.553
20	90	17.5	27.5	2.40	0.000	12.09	1.94	0.356
21	65	17.5	50.0	2.40	0.409	24.23	1.79	0.506
22	40	5.00	5.00	2.00	0.233	21.32	2.53	0.451
23	40	30.0	5.00	2.00	0.356	38.65	2.71	0.553
24	90	30.0	5.00	2.00	0.000	10.18	1.95	0.335
25	90	5.00	5.00	2.00	0.000	10.15	2.94	0.000
26	65	17.5	27.5	2.00	0.330	23.53	2.41	0.454
27	40	5.00	50.0	2.00	0.000	17.42	1.46	0.294
28	40	30.0	50.0	2.00	0.472	35.59	1.68	0.452
29	90	30.0	50.0	2.00	0.000	7.28	1.24	0.000
30	90	5.00	50.0	2.00	0.000	7.17	1.17	0.000
Optimum BWD values								
Working conditions	75.3	5.9	5.00	2.59				0.726
Calculated responses					0.52	35.6	3.49	
Experimental responses					0.49	31.7	3.67	

[a] Values in the eluent C, not in the mobile phase.

predicted and experimental values of the selected responses was also observed (Table 3), with a maximum deviation of around 10% for t_a, probably due to its dependency on a great number of variables (Fig. 1(b)). The optimum elution program starts with 2 min in isocratic conditions (23% A; 75% B; 2% C with 5 mM of ammonium formate at pH 2.6), then the percentage of B is linearly increased in 5.9 min up to 98% B (decreasing the percentage of eluent A accordingly and maintaining constant the 2% of eluent C). These isocratic conditions are maintained for 32 min; then ramped to original composition in 1 min, and equilibrated for 15 min.

The chromatogram obtained for the mixture of OH-PCBs on the HyPurity Advance column (amide-type) is shown in Fig. 3(a), where the elution order of the injected OH-PCBs is also identified. This result was compared in Fig. 3(b) with the chromatogram obtained with the method developed by Letcher et al. on an Ascentis C18 column [14]. As can be seen, this ODS-type column tends to separate the OH-PCBs mainly according to their molecular mass (correlated in this case with the number of chlorine atoms), whereas serious difficulties to separate homologous OH-PCBs were encountered. In fact, two OH-penta-CBs coelute almost completely, as also happens with the hepta-homologous 3′-OH-CB180 and 4-OH-CB187. Only OH-hexa-CBs are adequately resolved. This is a critical point, because these homologous compounds are indistinguishable by their m/z. However, the retention behavior of OH-PCBs in the amide-type column is quite different, because now those compounds with the same number of chlorine atoms have been separated in all the instances, avoiding the problem of isobaric interferences. Therefore, with regard to OH-PCBs separation, the amide-type column has shown to be clearly superior to the ODS-type, even being shorter in length.

Analytical performance of the optimized chromatographic method was evaluated by its repeatability (intra-day precision) and intermediate precision (inter-day precision). To calculate repeatability, expressed as relative standard deviation (RSD), six repeated injections of 10 μL of a methanol:water (70:30, v/v) OH-PCBs mixture (50 pg μL^{-1}) were carried out. The results obtained are detailed in Table 4. For the retention times, RSD values varied from 0.19 to 0.45%, while for peak areas values ranged from 1.9 to 8.5%. Intermediate precision was calculated from three replicate analyses of the above-mentioned solution but on three different days within a week. Thus, while RSD values of the retention times ranged from 0.12 to 1.1%, peak areas varied between 9.3 and 15%. Therefore, and according to these results, the performance of the chromatographic method optimized by BWD is adequate to carry out analyses of OH-PCBs with good robustness.

Table 4
Precision obtained with the chromatographic method developed by BWD to separate OH-PCBs in an amide-type column.

Compound	Repeatability (intra-day precision, RSD, %)		Intermediate precision (inter-day precision, RSD, %)	
	t_R	Area	t_R	Area
4-OH-CB107	0.37	4.5	0.28	15
4′-OH-CB108	0.34	8.5	0.24	15
3-OH-CB118	0.45	7.0	0.21	11
3′-OH-CB138	0.30	3.4	0.21	11
4-OH-CB146	0.28	2.2	0.27	9.3
4′-OH-CB159	0.31	5.0	0.12	12
4′-OH-CB172	0.29	3.1	0.35	13
3′-OH-CB180	0.33	2.2	0.19	12
4-OH-CB187	0.19	1.9	1.1	14

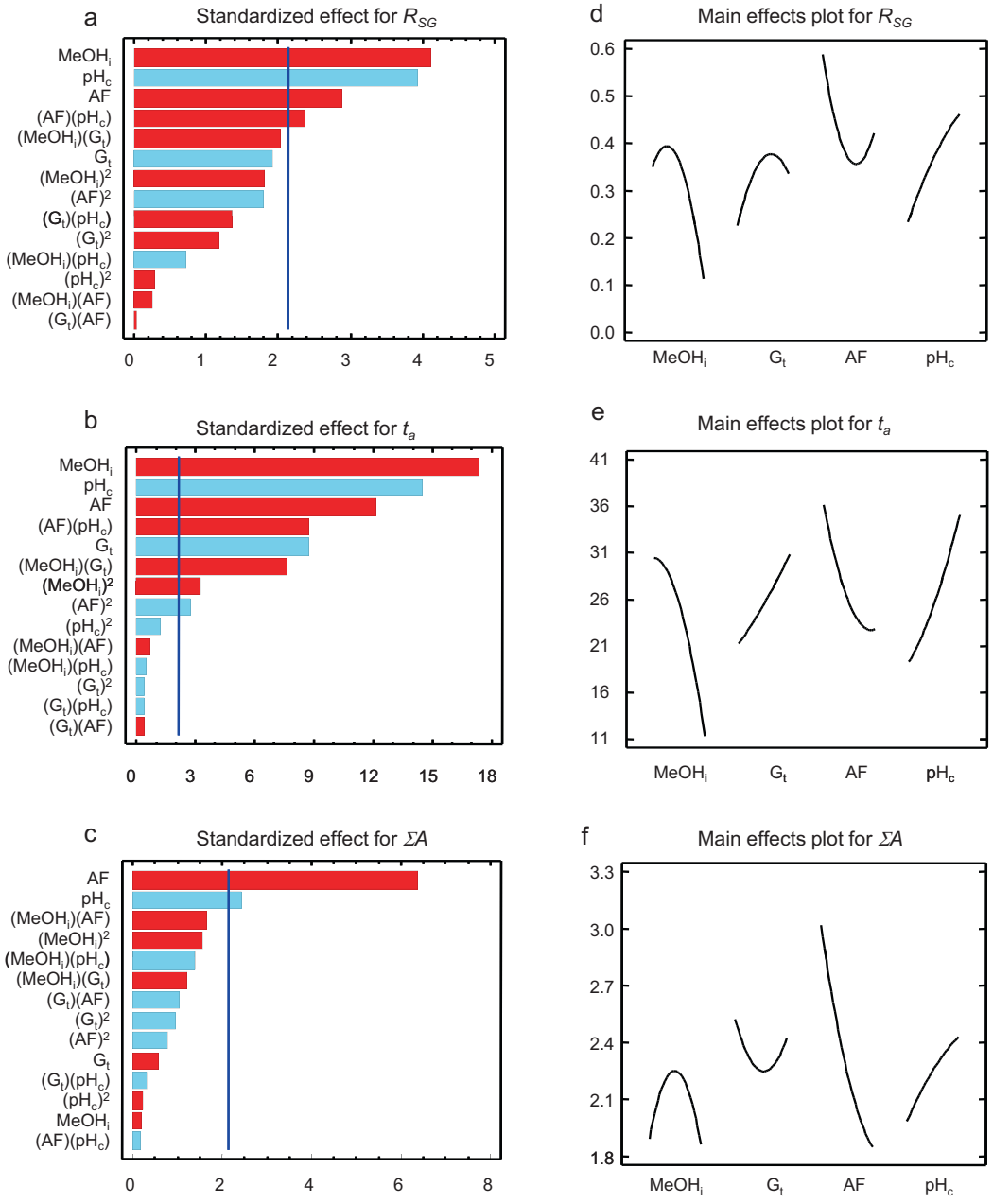

Fig. 1. Standardize Pareto charts (a–c) showing a vertical line corresponding to 5% of confidence level, and main effect plots (d–f). Both graphic types are shown for R_{SG} (a and d), t_a (b and e) and ΣA (c and f). Bars in blue (in light gray in the print version) or in red (in dark gray in the print version) indicate a positive or negative effect, respectively.

3.3. Retention modeling

As previously mentioned, the experimental design revealed that the relationship between experimental conditions and some chromatographic responses for the studied OH-PCBs seems to be quite complex in an amide-type column. For this reason, a deeper qualitative and quantitative knowledge of the interaction forces involved in the separation process of these compounds in an amide-type column could be of the greatest interest. However, it must be emphasized that it is not the intention of the authors to perform a detailed characterization, since it falls outside the aim of this study and several recent works has been published in this field [57,58].

In order to carry out the retention study, the molecular properties that could be easily obtained and correlated with the chromatographic elution were considered, bearing in mind that the studied SP is characterized by the presence of a hydrocarbon chain and an embedded amide group. Secondly, the ionizable nature of the OH-PCBs should also be considered, since the $[M-H]^-$ ion is the chemical species detected for each OH-PCB. Therefore, it seems reasonable to think that the two interaction forces that probably are involved in the retention to a greater degree are the dispersion forces between the apolar part of the analytes and the hydrocarbon chain of the SP, and the hydrogen bonds between the analyte hydroxyl group and the amide group of the SP. This reasoning was supported by the recent publication of Benhaim and Grushka [57], where an amide-type column (Ascentis RP-amide) was studied by applying the Abraham solvation parameter model [59]. The conclusion reached indicated that factors with the greatest influence in the chromatographic retention are related to the partition process and hydrogen bond generation. This criterion is also supported by the

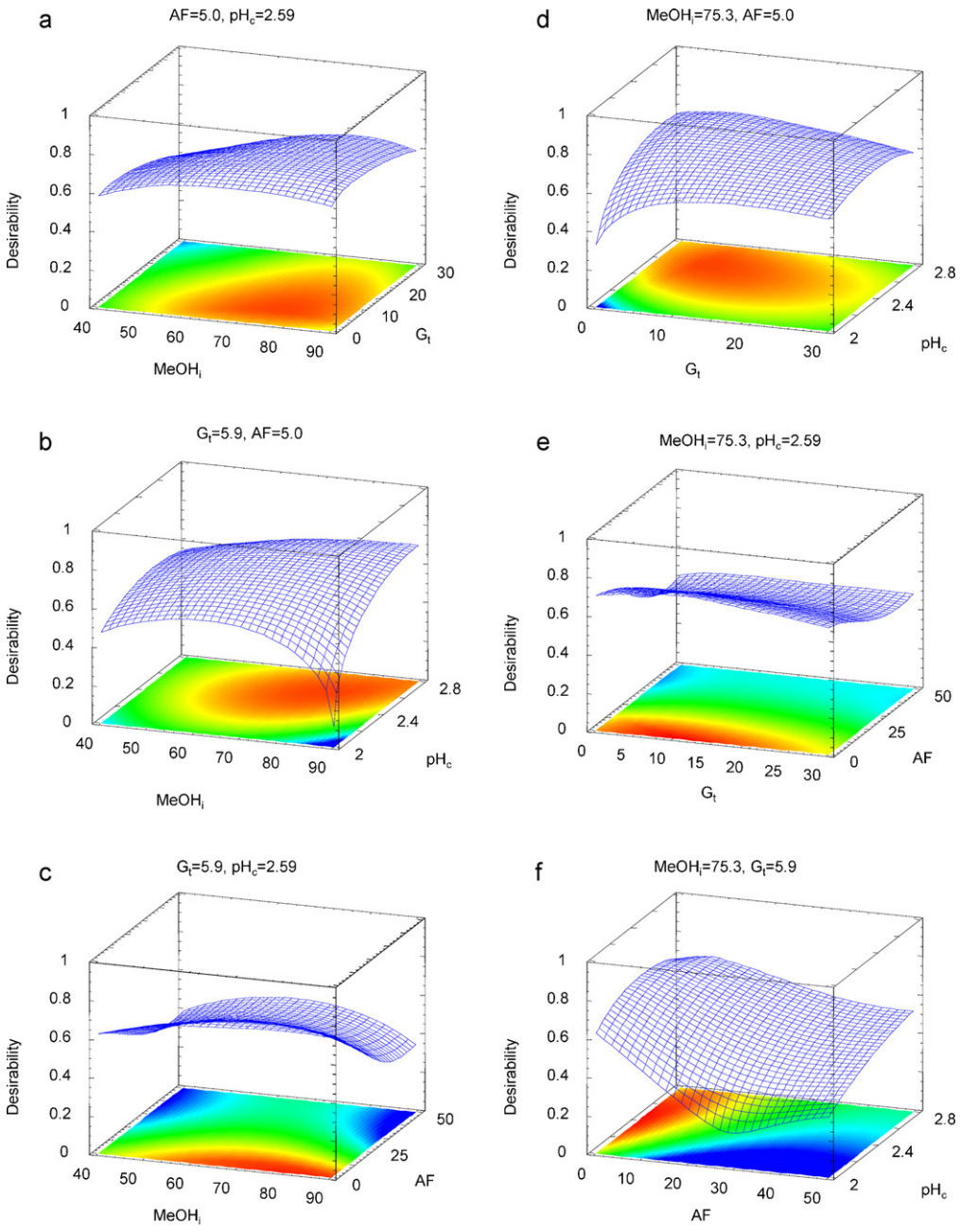

Fig. 2. Response surface plots showing the behavior of the desirability function against all the possible couples of variables used in the Box–Wilson design.

work carried out by other authors [29,30], where meticulous simulation of chromatographic retention is carried out on stationary phases for LC containing an embedded polar group, among them, a phase with an amide group. According to these authors, the prevailing forces in the chromatographic retention for this type of SPs are the hydrogen bonds, but the process seems not to be trivial at all. The reason is that when methanol is used as the eluent (as in the present study), it goes into the stationary phase and interacts by hydrogen bonds with the amide embedded group, generating an occluded methanol layer that takes an active role in the retention process. Although the expected hydrogen bonds between analyte molecules and the embedded amide groups were found, they are much more prevalent between analyte molecules and the methanol molecules in the occluded layer. In consequence, it really seems clear that the retention mechanism of the OH-PCBs in a column with an embedded amide group must be controlled by hydrogen bonds, with a certain contribution of dispersion forces, as had been supposed initially. However, from experiments in Section 3.2 it can be deduced that the relative contribution of both forces is not the same for the different OH-PCBs studied.

Therefore, the next step was to look for reliable molecular characteristics of the solutes related to the trend of giving hydrogen bond as well as dispersion interactions. Thus, the ability of a molecule to form hydrogen bonds is usually related to the strength or weakness of the acid character of their polar moiety, and the variables more successfully correlated with this property are the proton affinity of the molecule in gas phase or the logarithm of its acidity constant (pK_a) in liquid phase. With regards to the capacity of the solute to participate in dispersion interactions, it is usually correlated with the molecular volume (McGowan volume or equivalent), or from a more empirical point of view, with the logarithm of the partition coefficient ($\log P$), being defined for a given sub-

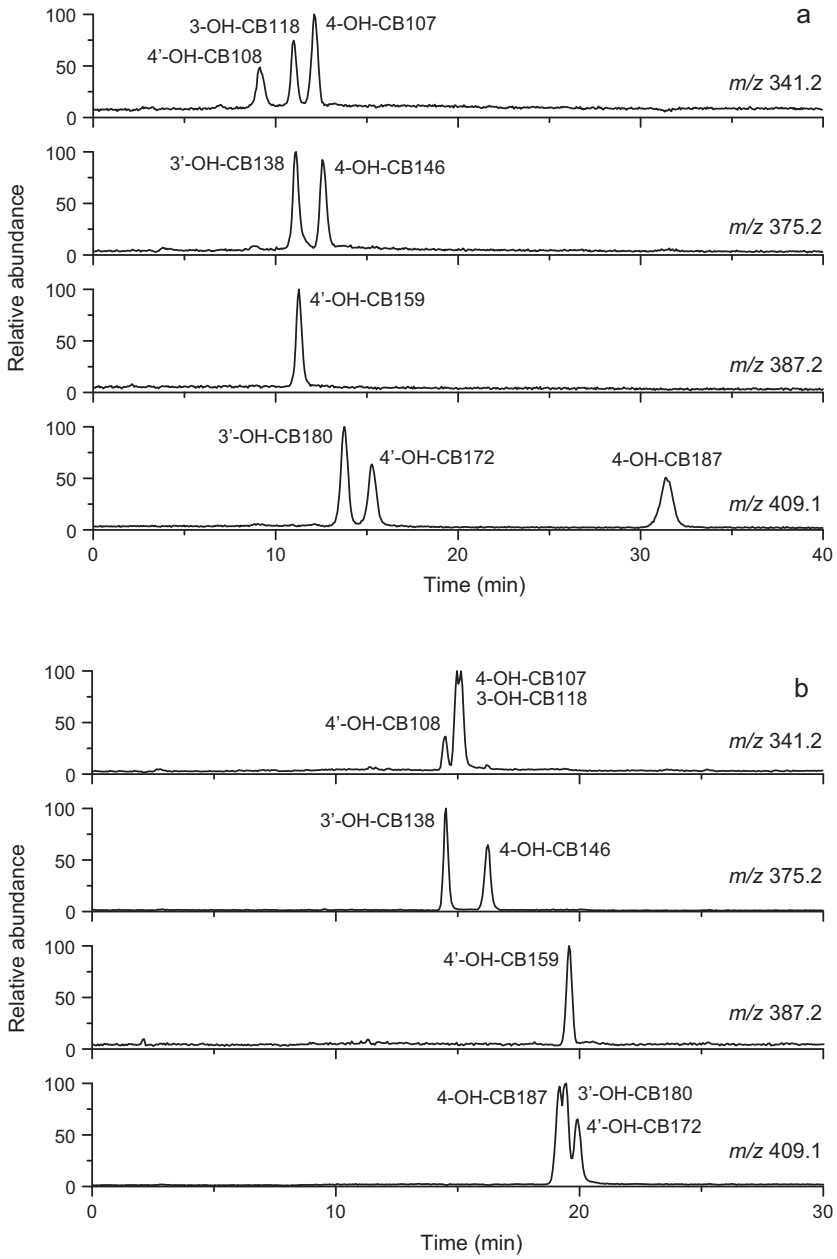

Fig. 3. Chromatograms obtained for the mixture of OH-PCBs in the (a) amide-type and (b) ODS-type columns.

stance as the ratio of its concentrations in the aqueous and organic phases. For ionizable substances, as in the case of OH-PCBs, log D should be used instead of log P, which was calculated using Eq. (2) as explained in Section 2.4.

Log D and pK_a were selected as the most suitable parameters to correlate with retention, and their values were obtained (Table 5). Then, the analysis of the OH-PCBs mixture under isocratic conditions was carried out, using percentages of methanol (φ) in the mobile phase ranging between 65 and 98%. A concentration of 0.1 mM of ammonium formate in the mobile phase was used in all the cases (2% of eluent C containing 5 mM of ammonium formate at pH 2.6). For this study, and for comparative purposes, apart from the amide-type column, an ODS-type column was also used, both with the same geometry. The retention factors (k) of the studied OH-PCBs were plotted against each φ value for both columns. Relevant information can be achieved from these plots, based on the Snyder solvent strength model, which is represented by Eq. (4).

$$\log k = \log k_w - S\varphi \quad (4)$$

First of all, the most outstanding fact was the different trends of these graphs in each chromatographic column. As an example, Fig. 4 shows these variations for 3′-OH-CB180, this tendency being equivalent for the rest of the studied compounds. The linearity for log k against φ in the ODS-type column is clear, with a value for the coefficient of determination (R^2) of 0.9985, whereas in the amide-type column an evident curvature is observed, with a lower value of R^2 (0.9760). This behavior is frequently found in chromatographic columns with polar stationary phases indicating a combined retention process [60,61].

The second conclusion that can be reached from the relationship between log k and φ comes from the smooth variation observed in plots of Fig. 4, where the absence of discontinuities can be veri-

Table 5
Calculated ${}^{s}_{w}pK_{\alpha}$ and log D values for OH-PCBs at each methanol percentage (φ).

φ	65	70	75	80	85	90	95	98
${}^{s}_{w}$pH	3.84	3.90	3.97	4.08	4.20	4.36	4.54	4.65
${}^{s}_{w}pK_{\alpha}$								
4-OH-CB107	5.31	5.27	5.23	5.19	5.14	5.08	5.03	4.98
4′-OH-CB108	6.43	6.43	6.43	6.44	6.46	6.46	6.47	6.48
3-OH-CB118	5.67	5.64	5.62	5.59	5.56	5.52	5.48	5.45
3′-OH-CB138	5.51	5.48	5.45	5.41	5.36	5.31	5.26	5.22
4-OH-CB146	5.17	5.13	5.08	5.03	4.97	4.91	4.83	4.78
4′-OH-CB159	6.32	6.33	6.33	6.33	6.33	6.33	6.33	6.34
4′-OH-CB172	5.08	5.03	4.97	4.92	4.85	4.78	4.69	4.64
3′-OH-CB180	5.41	5.37	5.33	5.28	5.23	5.17	5.11	5.07
4-OH-CB187	3.98	3.88	3.78	3.67	3.55	3.41	3.26	3.15
log D								
4-OH-CB107	6.32	6.32	6.31	6.31	6.29	6.26	6.22	6.17
4′-OH-CB108	5.71	5.71	5.71	5.71	5.71	5.71	5.71	5.71
3-OH-CB118	6.33	6.33	6.33	6.32	6.32	6.31	6.29	6.27
3′-OH-CB138	6.67	6.67	6.67	6.66	6.65	6.64	6.61	6.58
4′-OH-CB159	6.78	6.78	6.77	6.76	6.73	6.69	6.62	6.56
4-OH-CB146	6.90	6.90	6.90	6.90	6.90	6.90	6.90	6.89
4′-OH-CB172	7.37	7.36	7.35	7.34	7.31	7.26	7.16	7.09
3′-OH-CB180	7.38	7.38	7.38	7.37	7.36	7.33	7.29	7.25
4-OH-CB187	7.29	7.22	7.12	6.98	6.78	6.53	6.23	6.01

fied. This behavior implies that the steric effects do not contribute significantly to the retention process in the range of eluent composition assayed. This is an important point to consider because steric effects can have a relevant contribution to retention, especially at low organic solvent content in the mobile phase, as several authors have recently stated [62–64].

Finally, the k values of each OH-PCB in pure water (log k_w) can be obtained from Eq. (4), extrapolating the model at 100% of water in the mobile phase, that is from the y-intercept value. In this equation, the slope (S) depends on the solvent strength and is structurally correlated with the hydrophobic surface of the compound, hence with the dispersion interactions [60,65–67]. A linear relationship between log k_w and S for a group of compounds indicates a similar type of interaction involved in the retention of those compounds [68]. These plots can be seen in Fig. 5 for the ODS and the amide-type columns. In the case of the ODS column all the compounds are arranged in an almost perfect straight line, revealing that these OH-PCBs must be separated by the same mechanism, i.e. dispersion forces, the only possible interactions on ODS-type columns except for polar interactions with residual silanol groups. A different situation for the amide-type column was observed, since all the compounds are located in a straight line except for 4-OH-CB187 which is situated at a good distance from this line. This indicates that, in some way, the type of interaction that this compound undergoes with the stationary phase is different from the rest, which is curious since all of them have an almost identical structure.

In order to elucidate this point, plots of log k *vs.* log D and ${}^{s}_{w}pK_{a}$ for each OH-PCB were drawn at every mobile phase composition, because they should be related to the retention mechanisms by dispersion forces and hydrogen bonds, respectively. The R^2 values of these graphs, taken as an indicator of goodness of fit, are shown

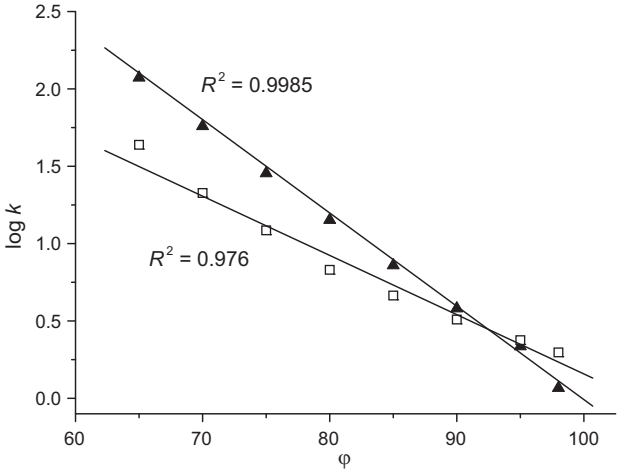

Fig. 4. Variation of log k *vs.* φ for 3′-OH-CB180 in the (□) amide-type and (▲) ODS-type columns.

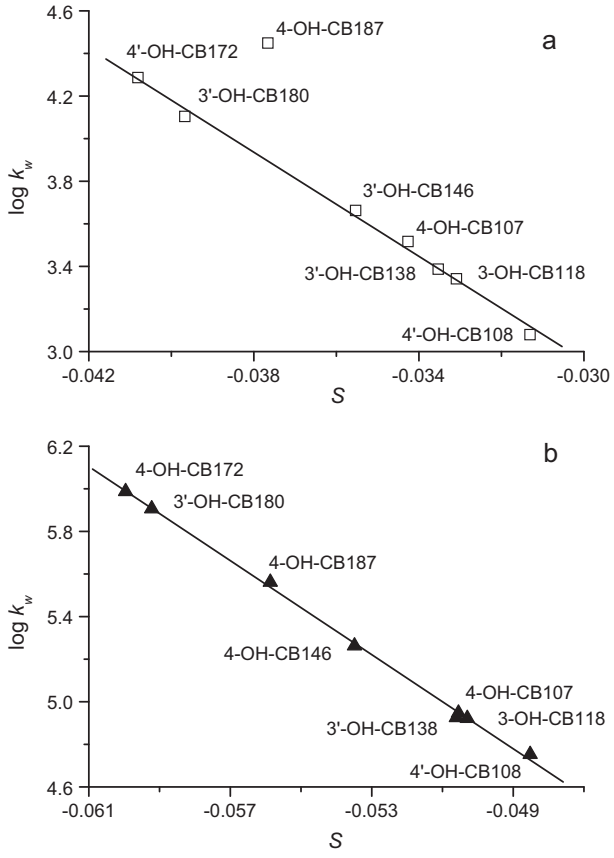

Fig. 5. Relationship between the Snyder model slope (S) and ordinate (log k_w) for OH-PCBs in the (a) amide-type and (b) ODS-type columns.

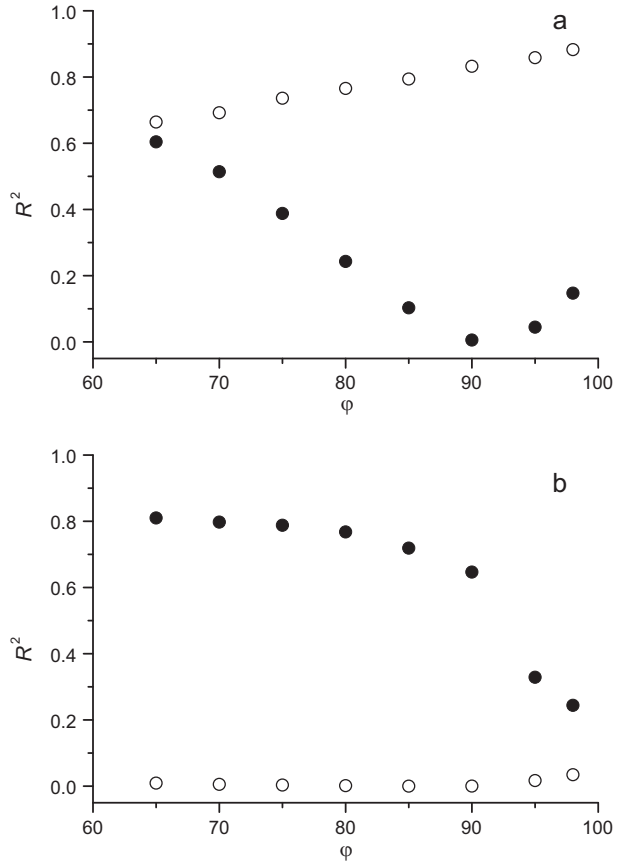

Fig. 6. Coefficient of determination values obtained for the relationships of (○) log k *vs.* ${}^{s}_{w}pK_a$ and (●) log k *vs.* log D in the (a) amide-type and (b) ODS-type columns.

in Fig. 6. As can be seen, in the amide-type column (Fig. 6(a)), the prevalent retention mechanism is due to interactions by hydrogen bonds, reaching values of R^2 between 0.65 and 0.9 for log k *vs.* ${}^{s}_{w}pK_a$ in the whole range of mobile phase composition studied. Nevertheless, the contribution of dispersion forces is also significant for the lower contents of methanol tested, with values of R^2 up to 0.6 for log k *vs.* log D. This double contribution to the retention mechanism allows modulating the separation of OH-PCBs, carrying out appropriate gradients of methanol. Thus, at low contents of methanol, OH-PCBs are mainly separated by their substitution degree (typical of the ODS-type columns) because of dispersion forces, and when moving to higher contents of methanol, where the predominant forces are the hydrogen bonds, the separation is driven by the ${}^{s}_{w}pK_a$ values of the compounds (Table 5).

With regards to the ODS-type column, Fig. 6(b) clearly shows that the retention mechanism is almost exclusively due to dispersion forces, with an R^2 value over 0.8 for log k *vs.* log D, whereas the correlation with the value of ${}^{s}_{w}pK_a$ is virtually zero. This behavior continues until the contents of methanol in the mobile phase exceed 90%. From this point a progressive decrease of the correlation for log k *vs.* log D takes place, indicating a great reduction in retention with very high organic modifier contents, making it difficult to set up solute-stationary phase interactions. In addition to all that stated above, in case of retention of ionizable substances on an amide-type column, a further experimental factor exists, namely the pH of the eluent, which can be used as an additional tool in the separation process. This fact has been clearly seen in the particular behavior of 4-OH-CB187 in Fig. 5, confirming the existence of some difference in its retention mechanism. This can be explained by its ${}^{s}_{w}pK_a$ value, the smallest among all the OH-PCBs studied (Table 5). As a consequence, the 4-OH-CB187 is the only OH-PCB virtually ionized at the working pH, causing the type of hydrogen bond that this compound undergoes with the amide-type stationary phase to be guided by a negative charge, and consequently this bond is much more intense than that of the remaining compounds [69–71]. In other words, the modification of the eluent pH gives an additional tool with which to control the strength of the hydrogen bonds of the studied OH-PCBs, and therefore their chromatographic retention in this type of columns.

All these results show the variety of retention mechanisms that ionizable compounds, like the studied OH-PCBs, can undergo with amide-type columns. In fact, this variety is responsible for the special selectivity of these stationary phases with regard to compounds with hydroxyl groups.

4. Conclusions

To sum up, after applying experimental design procedures, a liquid chromatographic method for the separation of OH-PCBs on an amide-type column has been developed, with very good resolution and sensitivity, and a reasonably short analysis time. The developed method allows all isobaric compounds tested in the mixture to be separated, this having proved quite difficult in an ODS column. A Response Surface Methodology was used for method optimization, applying a Box–Wilson Central Composite Design. The initial content of methanol in the mobile phase, the gradient time, and the concentration and the pH value of the buffer (ammonium formate/formic acid) were selected as relevant experimental parameters. A global optimum was obtained by using the Derringer's function value and selecting the elution time, the sensitivity and the overall resolution as responses to optimize. In addition, the retention study carried out revealed that the prevalent interaction between OH-PCBs and the amide-type SP takes place by hydrogen bonds, although dispersion forces also play an important role for moderate content of methanol in the mobile phase. Furthermore, the Snyder solvent strength model showed that the mobile phase pH value is the most important parameter in the control of the separation of OH-PCBs, since it allows modulation of the strength of the hydrogen bonds.

Acknowledgment

This study was supported by CSIC (project 200880I192), MICINN (project AGL2009-09733) and CAM (project S2009/AGR-1464)

References

[1] G.M. Frame, J.W. Cochran, S.S. Bowadt, J. High Resolut. Chromatogr. 19 (1996) 657.
[2] T. Sinjari, E. Klasson-Wehler, L. Hovander, P.O. Darnerud, Xenobiotica 28 (1998) 31.
[3] C.D. Sandau, P. Ayotte, E. Dewailly, J. Duffe, R.J. Norstrom, Environ. Health Perspect. 108 (2000) 611.
[4] R.J. Letcher, J.G. Lemmen, B. van der Burg, A. Brouwer, Å. Bergman, J.P. Giesy, M. van den Berg, Toxicol. Sci. 69 (2002) 362.
[5] A.C. Gutleb, P. Cenijn, M. van Velzen, E. Lie, E. Ropstad, J.U. Skaare, T. Malmberg, A. Bergman, G.W. Gabrielsen, J. Legler, Environ. Sci. Technol. 44 (2010) 3149.
[6] A.S. Mortensen, M. Braathen, M. Sandvik, A. Arukwe, Ecotoxicol. Environ. Saf. 68 (2007) 351.
[7] M. Braathen, A.S. Mortensen, M. Sandvik, J.U. Skåre, A. Arukwe, Arch. Environ. Contam. Toxicol. 56 (2009) 111.
[8] K. Haraguchi, Y. Kato, R. Kimura, Y. Masuda, Chem. Res. Toxicol. 11 (1998) 1508.
[9] R.J. Letcher, W.E. Klasson, Å. Bergman, in: J. Paasivirta (Ed.), Handbook of Environmental Chemistry. New Types of Persistent Halogenated Compounds, Park K, vol. 3, Springer-Verlag, Berlin, 2000, p. 315.
[10] H. Jörundsdóttir, A. Bignert, J. Svavarsson, T. Nygård, P. Weihe, Å. Bergman, Sci. Tot. Environ. 407 (2009) 4174.
[11] J.E. Hong, H. Pyo, S.-J. Park, W. Lee, J. Chromatogr. B 856 (2007) 1.
[12] S. Jensen, D. Lindqvist, L. Asplund, J. Agric. Food Chem. 57 (2009) 5872.
[13] U. Berger, D. Herzke, T.M. Sandanger, Anal. Chem. 76 (2004) 441.
[14] R.J. Letcher, H.X. Li, S.G. Chu, J. Anal. Toxicol. 29 (2005) 209.
[15] K. Tobiishi, H. Tsukatani, Organohalog. Compd. 70 (2008) 2309.
[16] H. Engelhardt, R. GrOner, M. Scherer, Chromatogr. Suppl. 53 (2001) S-154.

[17] J. Layne, J. Chromatogr. A 957 (2002) 149.
[18] C.R. Silva, I.C. Sales Fontes Jardim, C. Airoldi, J. Chromatogr. A 987 (2003) 139.
[19] M.R. Euerby, P. Petersson, J. Chromatogr. A 1088 (2005) 1.
[20] E. Lesellier, C. West, A. Tchapla, J. Chromatogr. A 1111 (2005) 62.
[21] J.W. Coym, J. Sep. Sci. 31 (2008) 1712.
[22] T.L. Ascah, B.J. Feibush, J. Chromatogr. 506 (1990) 357.
[23] C. Imaz, R. Navajas, D. Carreras, C. Rodríguez, A.F. Rodríguez, J. Chromatogr. A 870 (2000) 23.
[24] P. Viñas, C. López-Erroz, N. Balsalobre, M. Hernández-Córdoba, J. Chromatogr. A 1007 (2003) 77.
[25] Katell le Mapihan., 2004. Ph.D. Thesis. Université de Paris VI.
[26] R. Carabias-Martínez, E. Rodríguez-Gonzalo, N.W. Smith, L. Ruano-Miguel, Electrophoresis 27 (2006) 4423.
[27] D. Thiébaut, J. Vial, M. Michel, M.C. Hennion, T. Greibrokk, J. Chromatogr. A 1122 (2006) 97.
[28] Z.Q. Guo, D. Xu, Q.H. Wan, L. Chen, Chin. J. Anal. Chem. 37 (2009) 232.
[29] J.L. Rafferty, J.I. Siepmann, M.R. Schure, Anal. Chem. 80 (2008) 6214.
[30] J.L. Rafferty, J.I. Siepmann, M.R. Schure, J. Chromatogr. A 1216 (2009) 2320.
[31] A. Dean, D. Voss, Å. Bergman, in: G. Casella, S. Fienberg, I. Olkin (Eds.), Springer Texts in Statistics. Design and Analysis of Experiments, Springer-Verlag, New York, 1999, p. 764.
[32] C. Seto, K.P. Bateman, B. Gunter, J. Am. Soc. Mass Spectrom. 13 (2002) 2.
[33] A.C. Atkinson, R.D. Tobias, J. Chromatogr. A 1177 (2008) 1.
[34] I. Canals, J.A. Portal, E. Bosch, M. Rosés, Anal. Chem. 72 (2000) 1802.
[35] I. Canals, F.Z. Oumada, M. Rosés, E. Bosch, J. Chromatogr. A 911 (2001) 191.
[36] N. Garcia-Villar, J. Saurina, S. Hernández-Cassou, Anal. Chim. Acta 575 (2006) 97.
[37] S.C. Wang, H.J. Liao, W.C. Lee, C.M. Huang, T.H. Tsai, J. Chromatogr. A 1212 (2008) 68.
[38] C. Stalikas, Y. Fiamegos, V. Sakkas, T. Albanis, J. Chromatogr. A 1216 (2009) 175.
[39] R. Webb, P. Doble, M. Dawson, J. Chromatogr. B 877 (2009) 615.
[40] M.C. Breitkreitz, I.C.S.F. Jardim, R.E. Bruns, J. Chromatogr. A 1216 (2009) 1439.
[41] V.I. Boti, V.A. Sakkas, T.A. Albanis, J. Chromatogr. A 1216 (2009) 1296.
[42] M.A. Raji, K.A. Schug, Int. J. Mass Spectrom. 279 (2009) 100.
[43] R.H. Myers, D.C. Montgomery, Response Surface Methodology. Process and Product Optimization Using Design Experiments, 2nd ed., John Wiley & Sons, New York, 2002.
[44] S.L.C. Ferreira, R.E. Bruns, E.G. Paranhos da Silva, W.N. Lopes dos Santos, C.M. Quintella, J.M. David, J. Bittencourt de Andrade, M.C. Breitkreitz, I. Cristina, S.F. Jardim, B.B. Neto, J. Chromatogr. A 1158 (2007) 2.
[45] S.L.C. Ferreira, R.E. Bruns, H.S. Ferreira, G.D. Matos, J.M. David, G.C. Brandao, E.G.P. da Silva, L.A. Portugal, P.S. Reis, A.S. Souza, W.N.L. dos Santos, Anal. Chim. Acta 597 (2007) 179.
[46] V. Wsól, A.F. Fell, J. Biochem. Biophys. Methods 54 (2002) 377.
[47] M.R. Hadjmohammadi, P. Ebrahimi, Anal. Chim. Acta 516 (2004) 141.
[48] B. Jančić, M. Medenica, D. Ivanović, A. Malenović, Acta Chim. Slov 54 (2007) 49.
[49] Y. Zhou, J.Z. Song, F.F.K. Choi, H.F. Wu, C.F. Qiao, L.S. Ding, S.L. Gesang, H.X. Xu, J. Chromatogr. A 1216 (2009) 7013.
[50] P. Barmpalexis, F.I. Kanazeb, E. Georgarakis, J. Pharm. Biomed. Anal. 49 (2009) 1192.
[51] SPARC On-Line Calculator, University of Georgia, USA, http://ibmlc2.chem.uga.edu/sparc/.
[52] C. Liao, M.C. Nicklaus, J. Chem. Inf. Model. 49 (2009) 2801.
[53] E. Bosch, P. Bou, H. Allemann, M. Rosés, Anal. Chem. 68 (1996) 3651.
[54] G. Derringer, R. Suich, J. Qual. Technol. 12 (1980) 214.
[55] P. Ebrahimi, M.R. Hadjmohammadi, J. Chemometrics 21 (2007) 35.
[56] T. Sivakumar, R. Manavalan, C. Muralidharan, K. Valliappan, J. Pharm. Biomed. Anal. 43 (2007) 1842.
[57] D. Benhaim, E. Grushka, J. Chromatogr. A 1217 (2010) 65.
[58] D.V. McCalley, J. Chromatogr. A 1217 (2010) 3408.
[59] M.H. Abraham, Chem. Soc. Rev. 22 (1993) 73.
[60] K. Valkó, L.R. Snyder, J.L. Glajch, J. Chromatogr. A 656 (1993) 501.
[61] M. Liu, E.X. Chen, R. Ji, D. Semin, J. Chromatogr. A 1188 (2008) 255.
[62] C.F. Poole, H. Ahmed, W. Kiridena, C. DeKay, W.W. Koziol, Chromatographia 62 (2005) 553.
[63] C.F. Poole, W. Kiridena, C. DeKay, W.W. Koziol, R.D. Rosencrans, J. Chromatogr. A 1115 (2006) 133.
[64] S.N. Atapattu, C.F. Poole, Chromatographia 71 (2010) 185.
[65] N. Chen, Y. Zhang, P. Lu, J. Chromatogr. 633 (1993) 31.
[66] C. Giaginis, S. Theocharis, A. Tsantili-Kakoulidou, Anal. Chim. Acta 573 (2006) 311.
[67] C. Giaginis, S. Theocharis, A. Tsantili-Kakoulidou, J. Chromatogr. A 1166 (2007) 116.
[68] T. Braumann, J. Chromatogr. 373 (1986) 191.
[69] H.M. Lee, N.J. Singh, K.S. Kim, in: S.J. Grabowski (Ed.), Hydrogen Bonding: New Insights. Weak to Strong Hydrogen Bonds, Springer, Dordrecht, 2006, p. 519.
[70] P. Gilli, L. Pretto, G. Gilli, J. Mol. Struct. 844–845 (2007) 328.
[71] P. Gilli, L. Pretto, V. Bertolasi, G. Gilli, Acc. Chem. Res. 42 (2009) 33.